Published in final edited form as:
Dev Biol. 2009 November 1; 335(1): 253–262. doi:10.1016/j.ydbio.2009.07.033.

Evolution of early embryogenesis in rhabditid nematodes

Michael Brauchle[1,2], **Karin Kiontke**[1], **Philip MacMenamin**[1,2], **David H. A. Fitch**[1], and **Fabio Piano**[1,2,*]

[1]Department of Biology, New York University, New York, New York 10003, USA

[2]Center for Genomics and Systems Biology, New York University, New York, New York 10003, USA

Abstract

The cell biological events that guide early embryonic development occur with great precision within species but can be quite diverse across species. How these cellular processes evolve and which molecular components underlie evolutionary changes is poorly understood. To begin to address these questions, we systematically investigated early embryogenesis, from the one- to the four-cell embryo, in 34 nematode species related to *C. elegans*. We found 40 cell-biological characters that captured the phenotypic differences between these species. By tracing the evolutionary changes on a molecular phylogeny, we found that these characters evolved multiple times and independently of one another. Strikingly, all these phenotypes are mimicked by single-gene RNAi experiments in *C. elegans*. We use these comparisons to hypothesize the molecular mechanisms underlying the evolutionary changes. For example, we predict that a cell polarity module was altered during the evolution of the *Protorhabditis* group and show that PAR-1, a kinase localized asymmetrically in *C. elegans* early embryos, is symmetrically localized in the one-cell stage of *Protorhabditis* group species. Our genome-wide approach identifies candidate molecules—and thereby modules—associated with evolutionary changes in cell-biological phenotypes.

Keywords

Nematoda; *C. elegans*; embryogenesis; early development; phenotypic analysis; cell polarity; phenotypic plasticity

Introduction

A major goal of evolutionary developmental biology is to understand the mechanisms underlying phenotypic change (Gerhart and Kirschner, 1997; Hartwell et al., 1999; Wilkins, 2002). Here we focus on the evolutionary changes affecting cellular events such as the timing or orientation of cell divisions, or positioning of the mitotic spindle to generate daughter cells of different sizes. Such changes may alter adult forms or not. In either case, it is important to understand the molecular mechanisms underlying the evolution of these cell biological processes.

*Corresponding author: Fabio Piano, Phone: 212 998 3737, Fax: 212 995 3691 fp1@nyu.edu.

Author contributions. MB and FP designed and performed the experiments, analyzed the data and wrote the paper. KK and DHAF provided the molecular phylogeny ahead of publication, supplied the strains and helped with paper writing. PM developed the database.

Database containing all movies: www.rhevolution.org

Nematode embryos are well suited to analyze fundamental aspects of cell biological processes (for review see Félix, 1999; Goldstein, 2001; Malakhov, 1994; Schierenberg, 2006). With the advent of genome-wide functional studies directed at dissecting the molecular mechanisms underlying all visible aspects of early embryogenesis in *C. elegans*, it is now possible to ask more global questions about the evolutionary patterns during early embryogenesis. Here, we study the evolution of cell biological events in early embryogenesis within a group of rhabditid nematodes related to *C. elegans*.

Concentrating on rhabditid species is motivated by several factors. First, previous comparative analyses have already documented some rather striking differences in early embryogenesis between some of these species (reviewed in Félix, 1999; Goldstein, 2001; Malakhov, 1994; Schierenberg, 2006). The differences include mechanisms to establish the anterior-posterior axis in the one-cell embryo (Goldstein et al., 1998) and to assign cell fates (Wiegner and Schierenberg, 1998), or embryonic cell lineage patterns (Skiba and Schierenberg, 1992; Vangestel et al., 2008). Second, to analyze diversity in an evolutionary context, it is essential to have a good hypothesis of the phylogenetic relationships among the species studied. For rhabditid nematodes, such a phylogeny was recently published (Kiontke et al., 2007) and provides the framework to precisely map the evolutionary trajectories of phenotypic change. Third, these rhabditid nematodes are closely related to the exceptionally well-studied model organism *C. elegans.* Through comparisons of the cellular wild-type phenotypes observed in different rhabditid species with the phenotypes that arise in *C. elegans* through mutation or RNAi knockdown, we can derive clues for the possible molecular mechanisms that underlie the evolution of these cellular behaviors.

Decades of genetic analysis (Cowan and Hyman, 2004; Gönczy and Rose, 2005; Guo and Kemphues, 1996; Nigon et al., 1960) and several genome-scale RNAi analyses have revealed the genetic requirements for early embryonic processes in C. *elegans* (Fraser et al., 2000; Gönczy et al., 2000; Piano et al., 2000; Piano et al., 2002; Sönnichsen et al., 2005; Zipperlen et al., 2001). Combining the extensive phenotype data with co-expression or protein interaction data has led to an initial draft of the genetic architecture underlying early embryogenesis in *C. elegans* (Gunsalus et al., 2005; Sönnichsen et al., 2005). From these analyses a picture emerged in which groups of highly interconnected genes (modules and molecular machines) work in concert to drive specific cellular processes, e.g. cytokinesis, cell cycle progression, completion of meiosis, proper chromosome segregation, and polarity establishment (Gunsalus et al., 2005; Sönnichsen et al., 2005). By providing an initial map of the molecular genetic architecture underlying early embryogenesis in one species, these studies allow us to address the molecular mechanisms involved in the evolution of early embryogenesis within a group of related species.

Here, we systematically analyze cellular behaviors during early development in 34 species related to *C. elegans* and map them onto the species phylogeny. We find a high level of interspecific diversity, suggesting that cell biological events—while usually fixed within one species—evolve quite freely, leading to a high level of homoplasy (e.g. convergence) in our dataset. To explore potential molecular subnetworks in which evolutionary changes may have produced these differences in cellular behaviors, we compare the interspecific differences with gene-specific phenotypes from RNAi studies in *C. elegans.* We test and confirm one prediction derived from these comparisons.

Materials and Methods

Strains

The following rhabditid strains were used in this study: *Bursilla* sp. (PS1179), *C. brenneri* (CB5161), *C. briggsae* (PB800), *C. elegans* (N2, CB4856), *C. remanei* (EM464), *C.*

japonica (SB339), *Caenorhabditis* sp. 1 (SB341), *Caenorhabditis* sp. 2 (DF5070), *Caenorhabditis* sp. 3 (PS1010), *Caenorhabditis* sp. 5 (JU727), *Choriorhabditis dudichi* (SB122), *Cruznema tripartitum* (SB202), *Diploscapter* sp. (JU359), *Distolabrellus veechi* (DF5024), *Oscheius dolichuroides* (DF5018), *Oscheius myriophila* (DF5020), *Oscheius tipulae* (CEW1), *Pellioditis typica* (DF5025), *Pellioditis* sp. (JU274), *Pelodera strongyloides* (DF5022), *Pelodera teres* (EM437), *Phasmarhabditis* sp. (EM434), *Poikilolaimus oxycercus* (SB200), *Pristionchus pacificus* (PS312), *Protorhabditis* sp. (JB122), *Protorhabditis* sp. (SB208), *Rhabditis brassicae* (SB193), *Rhabditella axei* (DF5006), *Rhabditoides inermis* (SB328), *Rhabditoides inermiformis* (SB303), *Rhabditoides regina* (DF5012), *Rhabditis blumi* (DF5010), *Rhabditis* sp. (SB347), *Teratorhabditis palmarum* (DF5019). As an outgroup we used *Panagrellus redivivus* (PS1163).

Growth conditions, movie recordings, character and state definitions, species signatures

Strains were cultured at 20 °C using standard *C. elegans* conditions (Brenner, 1974). Time-lapse digital movies were captured essentially as described (Piano et al., 2000). In summary, gravid adults were cut directly on a coverslip in M9, transferred to a 2% agarose pad and imaged with DIC microscopy. In cases where embryos are laid at the one-cell stage (in JU359, JB122, PS1179) they were sometimes collected directly from the plate. The posterior end of the embryos was defined as that end where the smaller P_1 blastomere is located. Binary characters were defined after primary screens that identified phenotypic differences ("rhabditid character set"). We designate "not applicable" (white boxes in Fig. 2) for characters which depend on the presence of a first character in cases where that character is absent. To obtain species signatures, we analyzed at least five embryos per species for all 40 binary characters (Table S1, Fig. S1). The final character state was scored as "yes" or "no" if the majority (at least two-thirds) of the movies for a given species showed the respective state. Otherwise, it was scored as "intermediate/variable".

Database

All scorings can be found at www.rhevolution.org. This website consists of a set of Perl CGI scripts that dynamically generate the front-end HTML, interfacing with ACeDB which acts as the back-end database. It is hosted using Apache on a server running on Ubuntu Linux.

Character analysis, clustering and GO term analysis

We used the concentrated-changes test (Maddison and Maddison, 1989), now implemented in MacClade, to test for character dependencies of changing characters (38*37=1406 possible combinations in both directions). Simulations with sample size 1000 were used. Significant pairs are listed in Table S2.

Movie signatures were clustered with the TM4 package (Saeed et al., 2003), using hierarchical clustering with euclidian distance and average linking (Fig. S3).

The lists of the genes that have similar RNAi phenotypes in *C. elegans* were searched for overrepresentation of specific GO terms (Ashburner et al., 2000) using Funcassociate (Berriz et al., 2003) resulting in the reported p-values.

Comparisons with C. elegans *RNAi phenotypes*

To recover genes that phenocopy specific rhabditid characters by RNAi in *C. elegans*, we manually searched and rescreened publicly available movies at phenobank.org and RNAi.org using the rhabditid character set.

Antibody generation, PAR-1 cloning, RNAi and immunolocalizations

C. elegans anti-PAR-1 was raised against a protein fusion of the PAR-1 C-terminus (LVQ to LNL [44aa]) using the pMAL system (NEB). The following primers were used to clone this part of *par-1* from *Protorhabditis* sp. (JB122) and *Diploscapter* sp. (JU359): F: 5′-GACTCACTTGTNCARTGGGARATGGA-3′ R: 5′-ATTTTCGWNGCDATRTTYTTRAA-3′. *C. elegans par-6(RNAi*) was performed by feeding as previously described (Kamath et al., 2001). For immunolocalization, one-cell stage embryos of *Protorhabditis* sp.(JB122), *Diploscapter* sp. (JU359) and *Bursilla* sp. (PS1179) were collected directly from the plate. Primary (PAR-1 at 1:200 dilution [this study], 12G10(alpha-tubulin) at 1:5 [Developmental Studies Hybridoma Bank]) and secondary antibodies (1:200 dilution [Jackson ImmunoResearch]) were applied at 37°C in a humidity chamber overnight and for 4 hours, respectively, following standard procedures for *C. elegans* (freeze-cracking and methanol fixation) (Fernandez and Piano, 2006). Pictures were acquired on a Leica microscope using a Hamamatsu camera and a 100x lens. Openlab deconvolution and Adobe Photoshop software were used to process images.

Results and Discussion

Early embryonic events differ greatly between rhabditid species

Previous studies have shown that the early embryos of different nematode species develop in different ways (Félix, 1999; Goldstein, 2001; Goldstein et al., 1998; Malakhov, 1994; Schierenberg, 2006). To further explore this diversity in a systematic comparison, we analyzed the cellular behaviors of early embryonic development using time-lapse microscopy, following the procedure depicted in Figure 1. We selected 34 species representing most of the lineages within rhabditids and one representative of the outgroup. For each species, we obtained early embryos that are just completing meiosis or in which the pronuclei have not yet met and recorded the cell biological behaviors from the one-cell stage to the four-cell stage with DIC microscopy at high temporal resolution. We collected at least five recordings per species and more than 400 recordings overall.

To analyze the phenotypic diversity, we developed a controlled vocabulary describing 40 characters corresponding to obvious cellular behaviors (“phenotypes”) that vary across species (Fig. S1, Table S1). We scored each time-lapse recording using this “rhabditid character set” to describe the wild-type events observed in each species. To archive and distribute the raw time-lapse data, as well as the scoring of each recording, we developed an open-access Web database driven by an AceDB engine (Durbin and Thierry-Mieg, 1994), http://www.rhevolution.org. This site serves as a new repository for all embryonic recordings presented here and can be navigated using pointers from each species and their phylogenetic position.

As suggested by previous analyses focusing on one time point or on few species, we indeed found that the cellular behaviors in early embryogenesis show a high level of diversity across rhabditids (summarized and depicted in Figs. 2 and 3). To illustrate this diversity, we first describe a subset of early embryonic events in *C. elegans* (Cowan and Hyman, 2004; Gönczy and Rose, 2005; Nigon et al., 1960) and then point out the main differences we observed in other species. In *C. elegans* embryos, the polar bodies, which are extruded as meiosis completes, are found almost exclusively in association with the anterior side (Goldstein and Hird, 1996) (Fig. 3A, character 3 in Fig. 2). During this period, the entire membrane of the one-celled embryo is contractile (“ruffling”). However, soon after fertilization, which brings in the paternal DNA and attached centrosomes (Albertson, 1984) (Fig. 3D, character 7 in Fig. 2), contractility ceases asymmetrically starting in the posterior, resulting in a deep pseudocleavage in the middle of the embryo (Fig. 3G, character 8 in Fig. 2). These membrane

dynamics reflect actomyosin reorganization during the first cell cycle (Munro et al., 2004). The two pronuclei then coalesce and the zygote divides asymmetrically. One manifestation of the different cell identities at the two-cell stage is the round centrosome in the anterior AB blastomere, compared to the disc-shaped centrosome in the posterior P_1 blastomere (Fig. 3J; character 25 in Fig. 2). These different shapes are thought to be a consequence of different dynein-dynactin-dependent forces on the centrosomes (Severson and Bowerman, 2003). During the next round of cell division, AB always divides first (Fig. 3M; character 34 in Fig. 2) and perpendicular to the AP axis (Fig. 3P; character 36 in Fig. 2) while P_1 divides along the AP axis, leading to the typical rhomboidal blastomere arrangement at the four-cell stage.

When comparing the other species to *C. elegans*, we observe differences in all cellular events (Fig. 2). In *Rhabditella axei*, for example, a polar body is often associated with the future posterior side (Fig. 3B; character 5 in Fig. 2), not the anterior side as in *C. elegans,* suggesting changes in the establishment of polarity. Movies of *R. axei* from early embryogenesis to hatching (www.rhevolution.org) confirm this polarity reversal. More subtle events associated with a polarized embryo also differ between species. In some species, e.g. *Protorhabditis* sp. (JB122), membrane contractility does not cease asymmetrically (Fig. 3H). In addition, *Protorhabditis* sp. (JB122) and *Rhabditella axei*, among others, lack a pseudocleavage altogether (Fig. 3B, H). We also find three species, *Bursilla* sp. (PS1179, Fig. 3E), *Protorhabditis* sp. (JB122, Fig. 3H) and *Diploscapter* sp. (JU359), which lack one parental pronucleus (also see Lahl et al., 2006;Nigon, 1949). These species are likely to be parthenogenetic. Surprisingly, in *Bursilla* sp. (Fig. 3E), the centrosomes are initially detached from the pronucleus and only later associate with it. After the first division, most species (e.g. *Rhabditoides inermis*,Fig. 3K) differ from *C. elegans* in that they exhibit two round centrosomes, yet like in *C. elegans* the first cell division is asymmetric and the two blastomeres divide asynchronously, suggesting that they have acquired different identities as a result of the first division. Some changes alter cell-cell contacts or the relative timing of cell divisions in the earliest embryonic stages. For example, contrary to the sequence of events at the two-cell stage in *C. elegans*, in the *Protorhabditis* group, the smaller P_1 cell divides first (Fig. 3Q); in other species, e.g. *Oscheius myriophila*, the AB and P_1 cells divide at the same time (Fig. 3N). These types of differences have been seen before in species more distantly related to *C. elegans* (Dolinski et al., 2001;Malakhov, 1994;Schierenberg, 2006;Skiba and Schierenberg, 1992). *Protorhabditis* sp. (JB122) (Fig. 3Q) and other *Protorhabditis* group species show a striking change that leads to altered cell-cell contacts: both blastomeres divide along the AP axis (Dolinski et al., 2001), giving rise to a linear blastomere arrangement at the four-cell stage in which ABp and P_2 do not contact one another. In *C. elegans*, this contact is required for a well-studied cell-cell signaling event involving Notch pathway components (Mello et al., 1994), which thus cannot occur in the same way in *Protorhabditis* group species.

Characters evolve independently of one another

As a first step to analyze the time-lapse data, we performed hierarchical clustering of the signatures of all movies. As a rule, the signatures of multiple movies of one species clustered together, confirming that, despite some individual differences between embryos, character states are reproducible within one species (Fig. S3). To further explore the consistency of our scoring, we tested the effect of temperature and different strain origin on the species signatures. We found that neither condition caused major deviation from the consensus signatures (Fig. S2). The cluster analysis was also useful to point to characters which tend to associate with each other, e.g. pseudocleavage and cytoplasmatic flow (Fig. S3). Such character correlations can be due to coevolution of independent molecular mechanisms or to pleiotropy resulting from the effect of a single molecular mechanism on several characters. However, they can also be simply the result of relatedness, where several species share the same character states because they inherited them from a common ancestor. To separate characters correlated

because of common ancestry from those correlated for other reasons, we applied the phylogeny. Specifically, we tested for changes that occur together more frequently than expected by chance using the concentrated changes test implemented in MacClade (Maddison and Maddison, 1989;Maddison and Maddison, 2005). Mapping the characters onto the phylogeny revealed an astonishing degree of homoplasy (e.g. Fig S4B). Only in one of the 36 characters with both states present in more than one species is the distribution of character states consistent with a single evolutionary event (character 36 [Fig. 2 and Fig. S4A] evolved in the stem species of the *Protorhabditis* group). Despite the high level of homoplasy, evidence for correlated character changes is scarce. Of 1406 possible character pairs, only 75 showed significant ($p<0.05$) dependency in the concentrated changes test and no two characters overlap completely (Table S2). For example, symmetric ruffling in the one-cell stage (ruffling of the plasma membrane all around the cell; character 2 in Fig. 2) is correlated with the absence of cytoplasmic flow ($p=0.007$, character 11 in Fig. 2). In *C. elegans*, ruffling is asymmetric (the membrane becomes smooth on one side) and cytoplasmatic flow is observed . From *C. elegans*, it is known that membrane contractility and cytoplasmic flow are both dependent on proper actomyosin function (Hill and Strome, 1988;Shelton et al., 1999). Despite the genetic dependency between these two cellular behaviors in *C. elegans*, membrane contractility can also be decoupled from cytoplasmic flow in other species. For example, in *R. blumi* and *R. axei* we see asymmetric membrane ruffling but no cytoplasmic flow (Fig. 2). These results demonstrate that characters which are genetically tightly linked in the *C. elegans* one-cell embryo can nevertheless evolve independently. That is, the evolution of cellular processes during early embryogenesis in rhabditids is highly mosaic.

All phenotypes observed in rhabditids are phenocopied in C. elegans *RNAi experiments*

To begin to explore the molecular mechanisms that might underlie the evolution of early embryonic events, we compared the diversity across rhabditid species with data from genome-wide RNAi studies in *C. elegans*. For this analysis, we relied on the early embryonic recordings of RNAi treated animals that were already available online (Gönczy et al., 2000; Piano et al., 2000; Piano et al., 2002; Sönnichsen et al., 2005; Zipperlen et al., 2001). Most of these data are from RNAi experiments that lead, ultimately, to embryonic lethality in *C. elegans*. However, evolutionary changes in these genes or genetic pathways—such as slight developmental delays in expression—could similarly affect early-embryonic cell-biological processes without causing lethality. Using this rationale, we looked for specific phenotypes in these RNAi experiments that resemble the “rhabditid character set” and could reveal insights into the possible molecular mechanisms underlying the phenotypic changes across species. Remarkably, when we re-analyzed the available recordings for phenotypes that were different from *C. elegans* wild-type but similar to other species, we could identify phenocopy examples for every one of the 40 characters of our rhabditid character set (Fig. 3 C,F,I,L,O,R show representative cases; examples for all 40 rhabditid characters are shown in Fig. S1). These results show that single gene perturbations in one species are sufficient to uncover the phenotypic diversity seen across all 34 rhabditid species and suggest that this diversity may not require many genetic changes.

For some characters involved in changes across rhabditid species, we could identify all genes that cause similar RNAi phenotypes in *C. elegans* (Fig. 4) by performing exhaustive searches at the phenobank.org (Sönnichsen et al., 2005) and RNAi.org (Gunsalus et al., 2004) databases. Examples include the set of three genes (*sun-1*, *zyg-12*, F40H6.6) that, when knocked down by RNAi in *C. elegans*, phenocopy the “detached centrosome” character state (character 7, Fig. 3D-F). The protein product of *zyg-12* localizes to the nuclear periphery in *C. elegans* and directly anchors the centrosome to the nuclear envelope (Malone et al., 2003). We see a detached centrosome in two species, *Protorhabditis* sp. (JB122) and *Bursilla* sp. (PS1179). A larger set of 16 genes affect the “centrosome shape” character when knocked down in *C.*

elegans (Fig. 3J-L; character 25 in Fig. 2): two round centrosomes are seen at the two-cell stage, as opposed to one round and one disc-shaped centrosome seen in wild-type *C. elegans* embryos (Severson and Bowerman, 2003). This condition is seen in *R. inermis* (Fig. 3K) and in several other species (Fig. 2, character 25). Genes that give rise to this phenotype in *C. elegans* include *dyrb-1*, which affects the forces on astral microtubules that are responsible for centrosome shape (Couwenbergs et al., 2007), and genes that affect polarity such as *par-2*, which indirectly dictate centrosome shape (Severson and Bowerman, 2003). Another example involves the relative timing of blastomere divisions at the two-cell stage. The 21 genes in *C. elegans* whose RNAi phenotypes affect the "asynchrony" character (Fig. 3M-O; character 34 in Fig. 2) are overrepresented for the GO category "cyclin-dependent protein kinase activity" (p=0.003). The phenotype of these 21 RNAi experiments, synchronous divisions of AB and P_1, closely resembles the situation seen in five rhabditid species. A final example includes *pkc-3*, *par-6* and *par-3*. These genes are involved in polarity establishment and spindle orientation in *C. elegans* (Cowan and Hyman, 2004; Gönczy and Rose, 2005; Guo and Kemphues, 1996), and their RNAi and mutant phenotypes resemble the spindle orientation seen in species of the *Protorhabditis* group (Fig. 3P-R; character 36 in Fig. 2). Because of this remarkably close resemblance between phenotypes, these RNAi experiments identify groups of candidate genes in which evolutionary changes may have occurred. These candidate genes can now be tested in further experiments.

Testing candidates molecules: the PAR complex is likely to be involved in an evolutionary change in the Protorhabditis *group*

The comparison of wild type phenotypes across species with RNAi phenotypes in *C. elegans* identified the genes of the PAR complex as candidates for being involved in the evolutionary change in the AB spindle orientation in *Protorhabditis* group species (Fig. S4A). Uniquely among rhabditids, species in this group (*Protorhabditis* and *Diploscapter*) display a linear arrangement of blastomeres in the early four-cell stage (character 36, www.rhevolution.org (Dolinski et al., 2001)). Although the linear arrangement of the four cells could be due to several causes, the time-lapse recordings as well as immunofluorescence labeling using tubulin antibodies showed that the centrosome pair in *Protorhabditis* sp. (JB122) undergoes a 90° rotation before the mitotic spindle is set up in the AB blastomere (rhevolution.org and Fig. S5). The phylogenetic distribution of the AB rotation indicates that it occurred once in the stem species of the *Protorhabditis* group and that it is derived from a situation in which the spindle in AB does not rotate (as in *C. elegans*) (Fig. S4A). The direction of this evolutionary change may seem counterintuitive from a cell biological standpoint, since rotating a spindle requires the activity of many proteins (Guo and Kemphues, 1996;Hyman and White, 1987;Sönnichsen et al., 2005). However, mutational and RNAi studies also show that single gene perturbations can lead to such a dramatic change in *C. elegans* (Guo and Kemphues, 1996;Hyman and White, 1987;Sönnichsen et al., 2005).

In *C. elegans*, the AB spindle rotates ectopically in *par-3*, *par-6* or *pkc-3* mutant embryos (Etemad-Moghadam et al., 1995; Hung and Kemphues, 1999; Tabuse et al., 1998), suggesting that these molecules might be involved in the evolutionary change in the *Protorhabditis* lineage. The products of these genes physically interact and constitute the "anterior PAR complex". Extensive molecular epistatic analyses in *C. elegans* have shown that the reduction or loss of function of PAR-3, PAR-6 or PKC-3 proteins leads to an expansion of the localization domain of PAR-2 and PAR-1 (Fig. 5B), proteins that are otherwise restricted to the posterior half of the one-cell stage embryo (Fig. 5A) (Boyd et al., 1996; Guo and Kemphues, 1995).

The *C. elegans* data allowed us to predict that if the spindle rotation in *Protorhabditis* group species is caused by an altered activity of any of the anterior PAR proteins, the localization pattern of the conserved kinase PAR-1 would be altered in these species. To test this prediction,

we generated antibodies against a conserved C-terminal domain of PAR-1 (Fig. S6) and visualized the PAR-1 localization in *Diploscapter* sp. (JU359) and *Protorhabditis* sp. (JB122). Whereas the antibodies stained embryos of these species in an asymmetric pattern similar to *C. elegans* embryos beginning with the two-cell stage (Fig. 5E, F), the staining pattern at the one-cell stage was different. PAR-1 localized weakly all around the cortex of metaphase one-cell embryos and was not asymmetric (n>100, Fig. 5C, D). This pattern is never seen in wild-type *C. elegans*, but is reminiscent of PAR-1 localization in embryos with compromised activity of the anterior PAR complex (Fig. 5B) (Guo and Kemphues, 1995;Guo and Kemphues, 1996).

The PAR-1 localization pattern in *Protorhabditis* and *Diploscapter* is striking, because the PAR-1 ortholog is asymmetrically localized even in species as distantly related to *C. elegans* as *Drosophila melanogaster* (Shulman et al., 2000; Tomancak et al., 2000). These data show an association of a change in the localization of a putative kinase with a major evolutionary change in spindle orientation.

Symmetric localization of PAR-1 in the one-cell embryos of *Protorhabditis* group species, however, does not mean that polarity is not established until after this stage. Indeed, several pieces of data support the idea that the first cell division in *Protorhabditis* group species is a bona fide asymmetric cell division: In *Protorhabditis* sp (JB122) a polar body is always found on the future posterior side (Fig. 5D), at the two-cell stage the anterior blastomere is always larger (Fig. 5E), and the second division is asynchronous (though in reverse order compared to *C. elegans*, www.rhevolution.org). In addition, laser ablations in *Protorhabditis* sp (JB122) show that the gut lineage (identified by the presence of birefringent gut granules) is produced only from P_1 and not from AB (n=3 for each case, Fig. S7). It is noteworthy that PAR-1 becomes asymmetrically localized in *Protorhabditis* group species beginning with the two-cell stage, and the embryos develop with obvious cell polarities. From these observations it seems likely that separate mechanisms exist for setting up polarity in the one-cell embryo vs. the later P-lineage. Consistent with this idea, in *C. elegans* the reestablishment of PAR protein asymmetry in P_2 requires proteins such as OOC-3 and OOC-5, which do not appear to play a role in establishing polarity at the one-cell stage (Basham and Rose, 1999).

Conclusion

In this study, we analyzed 40 cell biological phenotypes during early embryogenesis and found that during evolution almost all of them changed multiple times and independently of each other. Such a mosaic evolutionary pattern argues that the majority of the underlying molecular mechanisms are quite specific, affecting only some aspect of the cellular behaviors.

The pattern emerging from the comparison of phenotypes in different species complements the current view of the genetic architecture underlying early embryogenesis in *C. elegans*. Large-scale analyses have proposed that groups of genes which give rise to similar phenotypes upon mutation or RNAi often encode proteins that interact with each other physically, suggesting that molecular machines or modules drive early embryonic processes (Gunsalus et al., 2005; Piano et al., 2002; Walhout et al., 2002). Considering the evolutionary patterns, such a modular architecture could enable parts of the network to change independently of other modules, affecting only specific phenotypes without affecting the entire network. In addition, a specific module could be altered through changes in different genes with the same phenotypic outcome, thus providing a possible explanation for the high level of homoplasy we observed in our dataset. The idea that cellular functions are mediated by discrete sets of interacting molecules, or modules, and that such a modular architecture may facilitate evolutionary change, have been advanced previously (Hartwell et al., 1999). A modular architecture allows adaptability through changes in linkages between modules.

The approach presented here offers new possibilities to examine the molecular mechanisms that give rise to the remarkable array of phenotypic differences in early embryogenesis across nematodes and highlights how natural diversity can provide new insights into the evolution of a highly conserved system, such as the PAR module.

Supplementary Material

Refer to Web version on PubMed Central for supplementary material.

Acknowledgments

We thank G. Yucel, C. Roehrig, T. Hadi and M. Mana for helping with DIC recordings. We thank K. Gunsalus, M. Siegal and A. Fernandez for comments on the manuscript, as well as the Piano and Gunsalus labs and A. Ochoa-Espinosa for discussions. This work was supported by grants from NIH to F.P. (R01HD046236) and from HFSP (RGP0016/2001-M) and NSF (0228692, 0735230) to D.H.A.F.

References

Albertson DG. Formation of the first cleavage spindle in nematode embryos. Dev. Biol 1984;101:61–72. [PubMed: 6692980]

Ashburner M, Ball CA, Blake JA, Botstein D, Butler H, Cherry JM, Davis AP, Dolinski K, Dwight SS, Eppig JT, Harris MA, Hill DP, Issel-Tarver L, Kasarskis A, Lewis S, Matese JC, Richardson JE, Ringwald M, Rubin GM, Sherlock G. Gene ontology: tool for the unification of biology. The Gene Ontology Consortium. Nat. Genet 2000;25:25–29. [PubMed: 10802651]

Basham SE, Rose LS. Mutations in *ooc-5* and *ooc-3* disrupt oocyte formation and the reestablishment of asymmetric PAR protein localization in two-cell *Caenorhabditis elegans* embryos. Dev. Biol 1999;215:253–263. [PubMed: 10545235]

Berriz GF, King OD, Bryant B, Sander C, Roth FP. Characterizing gene sets with FuncAssociate. Bioinformatics 2003;19:2502–2504. [PubMed: 14668247]

Boyd L, Guo S, Levitan D, Stinchcomb DT, Kemphues KJ. PAR-2 is asymmetrically distributed and promotes association of P granules and PAR-1 with the cortex in *C. elegans* embryos. Development 1996;122:3075–3084. [PubMed: 8898221]

Brenner S. The genetics of *Caenorhabditis elegans*. Genetics 1974;77:71–94. [PubMed: 4366476]

Couwenbergs C, Labbe JC, Goulding M, Marty T, Bowerman B, Gotta M. Heterotrimeric G protein signaling functions with dynein to promote spindle positioning in *C. elegans*. J. Cell Biol 2007;179:15–22. [PubMed: 17908918]

Cowan CR, Hyman AA. Asymmetric cell division in *C. elegans*: cortical polarity and spindle positioning. Annu. Rev. Cell Dev. Biol 2004;20:427–453. [PubMed: 15473847]

Dolinski C, Baldwin JG, Thomas WK. Comparative survey of early embryogenesis of Secernentea (Nematoda), with phylogenetic implications. Can. J. Zoolg 2001;79:82–94.

Durbin, R.; Thierry-Mieg, J. The AceDB Genome Database. In: Shuhai, S., editor. Computational Methods In Genome Research. Plenum Press; New York: 1994. p. 45-55.

Etemad-Moghadam B, Guo S, Kemphues KJ. Asymmetrically distributed PAR-3 protein contributes to cell polarity and spindle alignment in early *C. elegans* embryos. Cell 1995;83:743–752. [PubMed: 8521491]

Félix MA. Evolution of developmental mechanisms in nematodes. J. Exp. Zool 1999;285:3–18. [PubMed: 10327646]

Fernandez AG, Piano F. MEL-28 is downstream of the Ran cycle and is required for nuclear-envelope function and chromatin maintenance. Curr. Biol 2006;16:1757–1763. [PubMed: 16950115]

Fraser AG, Kamath RS, Zipperlen P, Martinez-Campos M, Sohrmann M, Ahringer J. Functional genomic analysis of *C. elegans* chromosome I by systematic RNA interference. Nature 2000;408:325–330. [PubMed: 11099033]

Gerhart, J.; Kirschner, M. Cells, Embryos, and Evolution: Toward a Cellular and Developmental Understanding of Phenotypic Variation and Evolutionary Adaptability. Blackwell Publishers; Malden, MA: 1997.

Goldstein B. On the evolution of early development in the Nematoda. Philos. Trans. R. Soc. Lond. B Biol. Sci 2001;356:1521–1531. [PubMed: 11604120]

Goldstein B, Frisse LM, Thomas WK. Embryonic axis specification in nematodes: evolution of the first step in development. Curr. Biol 1998;8:157–160. [PubMed: 9443914]

Goldstein B, Hird SN. Specification of the anteroposterior axis in *Caenorhabditis elegans*. Development 1996;122:1467–1474. [PubMed: 8625834]

Gönczy P, Echeverri C, Oegema K, Coulson A, Jones SJ, Copley RR, Duperon J, Oegema J, Brehm M, Cassin E, Hannak E, Kirkham M, Pichler S, Flohrs K, Goessen A, Leidel S, Alleaume AM, Martin C, Ozlu N, Bork P, Hyman AA. Functional genomic analysis of cell division in *C. elegans* using RNAi of genes on chromosome III. Nature 2000;408:331–336. [PubMed: 11099034]

Gönczy, P.; Rose, LS. Asymmetric cell division and axis formation in the embryo. In: The *C. elegans* Research Community. , editor. WormBook. 2006. WormBook, doi/10.1895/wormbook.1.30.1

Gunsalus KC, Ge H, Schetter AJ, Goldberg DS, Han JD, Hao T, Berriz GF, Bertin N, Huang J, Chuang LS, Li N, Mani R, Hyman AA, Sonnichsen B, Echeverri CJ, Roth FP, Vidal M, Piano F. Predictive models of molecular machines involved in *Caenorhabditis elegans* early embryogenesis. Nature 2005;436:861–5. [PubMed: 16094371]

Gunsalus KC, Yueh WC, MacMenamin P, Piano F. RNAiDB and PhenoBlast: web tools for genome-wide phenotypic mapping projects. Nucleic Acids Res 2004;32:D406–D410. [PubMed: 14681444]

Guo S, Kemphues KJ. *par-1*, a gene required for establishing polarity in *C. elegans* embryos, encodes a putative Ser/Thr kinase that is asymmetrically distributed. Cell 1995;81:611–620. [PubMed: 7758115]

Guo S, Kemphues KJ. Molecular genetics of asymmetric cleavage in the early *Caenorhabditis elegans* embryo. Curr. Opin. Genet. Dev 1996;6:408–415. [PubMed: 8791533]

Hartwell LH, Hopfield JJ, Leibler S, Murray AW. From molecular to modular cell biology. Nature 1999;402:C47–C52. [PubMed: 10591225]

Hill DP, Strome S. An analysis of the role of microfilaments in the establishment and maintenance of asymmetry in *Caenorhabditis elegans* zygotes. Dev. Biol 1988;125:75–84. [PubMed: 3275427]

Hung TJ, Kemphues KJ. PAR-6 is a conserved PDZ domain-containing protein that colocalizes with PAR-3 in *Caenorhabditis elegans* embryos. Development 1999;126:127–135. [PubMed: 9834192]

Hyman AA, White JG. Determination of cell division axes in the early embryogenesis of *Caenorhabditis elegans*. J. Cell Biol 1987;105:2123–2135. [PubMed: 3680373]

Kamath RS, Martinez-Campos M, Zipperlen P, Fraser AG, Ahringer J. Effectiveness of specific RNA-mediated interference through ingested double-stranded RNA in *Caenorhabditis elegans*. Genome Biol 2001;2RESEARCH2.1-2.10

Kemphues K. PARsing embryonic polarity. Cell 2000;101:345–348. [PubMed: 10830161]

Kiontke K, Barrière A, Kolotuev I, Podbilewicz B, Sommer RJ, Fitch DHA, Félix MA. Trends, stasis and drift in the evolution of nematode vulva development. Curr. Biol 2007;17:1925–1937. [PubMed: 18024125]

Lahl V, Sadler B, Schierenberg E. Egg development in parthenogenetic nematodes: variations in meiosis and axis formation. Int. J. Dev. Biol 2006;50:393–398. [PubMed: 16525934]

Maddison WP, Maddison DR. Interactive analysis of phylogeny and character evolution using the computer program MacClade. Folia Primatol 1989;53:190–202. [PubMed: 2606395]

Maddison, WP.; Maddison, DR. MacClade 4.08 - Analysis of phylogeny and character evolution. Sinauer Associates; Sunderland, MA: 2005.

Malakhov, VV. Nematodes: structure, development, classification, and phylogeny. Smithsonian Institution Press; Washington, DC: 1994.

Malone CJ, Misner L, Le Bot N, Tsai MC, Campbell JM, Ahringer J, White JG. The *C. elegans* hook protein, ZYG-12, mediates the essential attachment between the centrosome and nucleus. Cell 2003;115:825–836. [PubMed: 14697201]

Mello CC, Draper BW, Priess JR. The maternal genes *apx-1* and *glp-1* and establishment of dorsal-ventral polarity in the early *C. elegans* embryo. Cell 1994;77:95–106. [PubMed: 8156602]

Munro E, Nance J, Priess JR. Cortical flows powered by asymmetrical contraction transport PAR proteins to establish and maintain anterior-posterior polarity in the early *C. elegans* embryo. Dev Cell 2004;7:413–424. [PubMed: 15363415]

Nigon V. Les modalités de la reproduction et déterminisme du sexe chez quelques nematodes libres. Ann. Sci. nat. Zool 1949;11:1–132.

Nigon V, Guerrier P, Monin H. L'architecture polaire de l'oeuf et les mouvements des constituants cellulaires au cours des premières étapes du développement chez quelques nématodes. Bull. Biol. Fr. Belg 1960;94:131–202.

Piano F, Schetter AJ, Mangone M, Stein L, Kemphues KJ. RNAi analysis of genes expressed in the ovary of *Caenorhabditis elegans*. Curr. Biol 2000;10:1619–1622. [PubMed: 11137018]

Piano F, Schetter AJ, Morton DG, Gunsalus KC, Reinke V, Kim SK, Kemphues KJ. Gene clustering based on RNAi phenotypes of ovary-enriched genes in *C. elegans*. Curr. Biol 2002;12:1959–1964. [PubMed: 12445391]

Saeed AI, Sharov V, White J, Li J, Liang W, Bhagabati N, Braisted J, Klapa M, Currier T, Thiagarajan M, Sturn A, Snuffin M, Rezantsev A, Popov D, Ryltsov A, Kostukovich E, Borisovsky I, Liu Z, Vinsavich A, Trush V, Quackenbush J. TM4: a free, open-source system for microarray data management and analysis. Biotechniques 2003;34:374–378. [PubMed: 12613259]

Schierenberg, E. Embryological variation during nematode development. In: The *C. elegans* Research Community. , editor. WormBook. 2006. p. 1-13.WormBook, doi/10.1895/wormbook.1.55.1

Severson AF, Bowerman B. Myosin and the PAR proteins polarize microfilament-dependent forces that shape and position mitotic spindles in *Caenorhabditis elegans*. J. Cell Biol 2003;161:21–26. [PubMed: 12695495]

Shelton CA, Carter JC, Ellis GC, Bowerman B. The nonmuscle myosin regulatory light chain gene *mlc-4* is required for cytokinesis, anterior-posterior polarity, and body morphology during *Caenorhabditis elegans* embryogenesis. J. Cell Biol 1999;146:439–451. [PubMed: 10427096]

Shulman JM, Benton R, Johnston D. The *Drosophila* homolog of *C. elegans* PAR-1 organizes the oocyte cytoskeleton and directs oskar mRNA localization to the posterior pole. Cell 2000;101:377–388. [PubMed: 10830165]

Skiba F, Schierenberg E. Cell lineages, developmental timing, and spatial pattern formation in embryos of free-living soil nematodes. Dev. Biol 1992;151:597–610. [PubMed: 1601187]

Sönnichsen B, Koski LB, Walsh A, Marschall P, Neumann B, Brehm M, Alleaume AM, Artelt J, Bettencourt P, Cassin E, Hewitson M, Holz C, Khan M, Lazik S, Martin C, Nitzsche B, Ruer M, Stamford J, Winzi M, Heinkel R, Roder M, Finell J, Hantsch H, Jones SJ, Jones M, Piano F, Gunsalus KC, Oegema K, Gönczy P, Coulson A, Hyman AA, Echeverri CJ. Full-genome RNAi profiling of early embryogenesis in *Caenorhabditis elegans*. Nature 2005;434:462–469. [PubMed: 15791247]

Tabuse Y, Izumi Y, Piano F, Kemphues KJ, Miwa J, Ohno S. Atypical protein kinase C cooperates with PAR-3 to establish embryonic polarity in *Caenorhabditis elegans*. Development 1998;125:3607–3614. [PubMed: 9716526]

Tomancak P, Piano F, Riechmann V, Gunsalus KC, Kemphues KJ, Ephrussi A. A *Drosophila melanogaster* homologue of *Caenorhabditis elegans par-1* acts at an early step in embryonic-axis formation. Nat. Cell Biol 2000;2:458–460. [PubMed: 10878812]

Vangestel S, Houthoofd W, Bert W, Borgonie G. The early embryonic development of the satellite organism *Pristionchus pacificus*: differences and similarities with *Caenorhabditis elegans*. Nematology 2008;10:301–312.

Walhout AJ, Reboul J, Shtanko O, Bertin N, Vaglio P, Ge H, Lee H, Doucette-Stamm L, Gunsalus KC, Schetter AJ, Morton DG, Kemphues KJ, Reinke V, Kim SK, Piano F, Vidal M. Integrating interactome, phenome, and transcriptome mapping data for the *C. elegans* germline. Curr. Biol 2002;12:1952–1958. [PubMed: 12445390]

Wiegner O, Schierenberg E. Specification of gut cell fate differs significantly between the nematodes Acrobeloides nanus and *Caenorhabditis elegans*. Dev. Biol 1998;204:3–14. [PubMed: 9851839]

Wilkins, AS. The evolution of developmental pathways. Sinauer Associates; Sunderland, MA: 2002.

Zipperlen P, Fraser AG, Kamath RS, Martinez-Campos M, Ahringer J. Roles for 147 embryonic lethal genes on *C.elegans* chromosome I identified by RNA interference and video microscopy. Embo J 2001;20:3984–3992. [PubMed: 11483502]

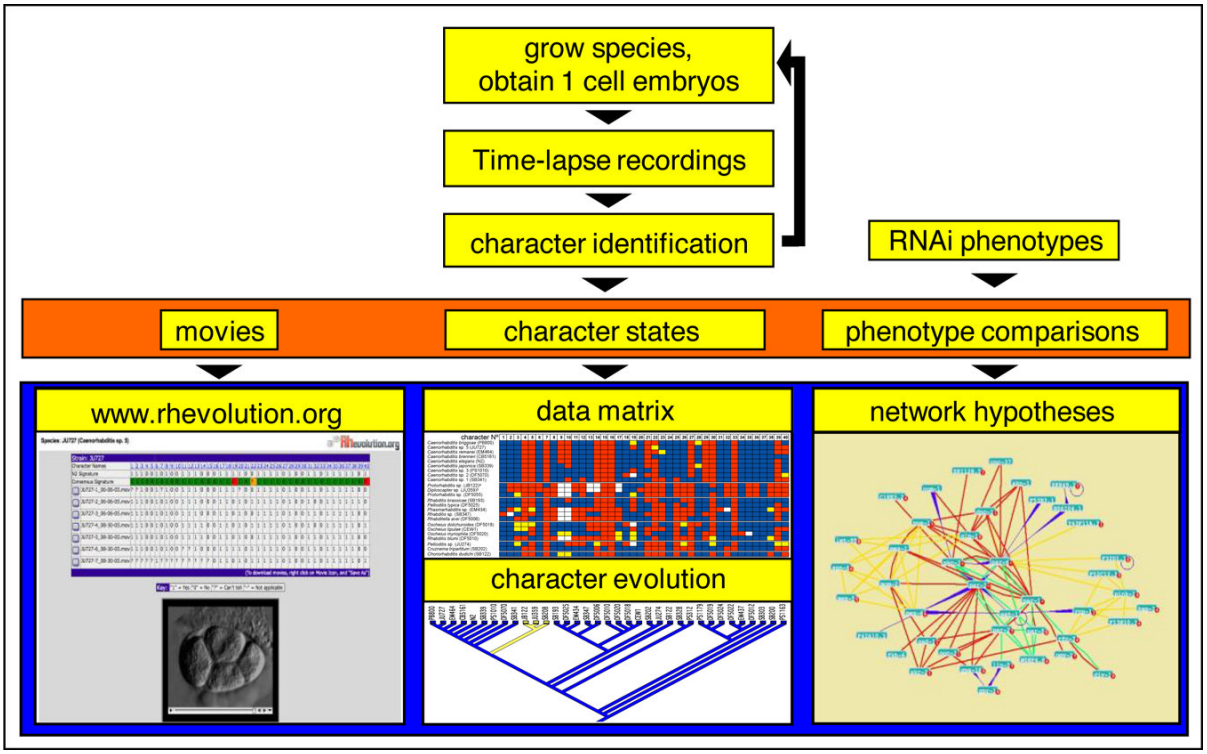

Figure 1. Overview of the phenotypic analyses and their results across rhabditid species

Data collection steps are indicated on top. The scheme was repeated until every character in every species had been scored at least five times. In addition to our movie analyses, we also reanalyzed published RNAi phenotypes from *C. elegans*. This resulted in a collection of movies of 35 species, 40 binary characters as well as RNAi phenotypes with which we could compare our data (orange box). Data analyses and processing steps then resulted in a database, the data matrix, character evolution analyses and network hypotheses (blue box).

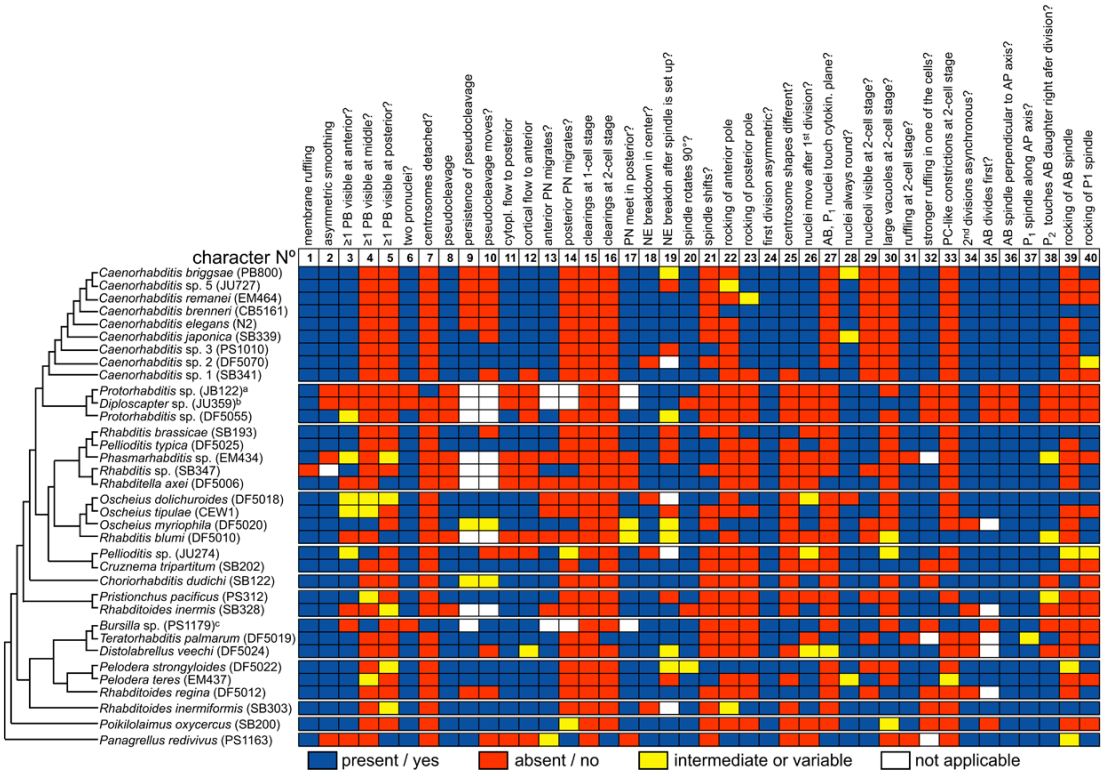

Figure 2. Phenotypic differences in early embryogenesis between 34 rhabditid species

Graphical representation of the distribution of the 40 binary rhabditid characters in 34 rhabditid species and *Panagrellus redivivus* as representative of the outgroup. Character states are color-coded as specified in the key. If less than two thirds of the screened embryos showed the same character state, the character was scored as variable and the cell is marked in yellow. On the left, a phylogenetic tree shows the relationships of the species (Kiontke et al., 2007). Characters are described in detail in Fig. S1 and at www.rhevolution.org. PB = polar body, PN = pronucleus, PC = pseudocleavage, NE = nuclear envelope.

[a] No polar bodies are seen by DIC in JB122 (characters 3-5). However, DAPI staining shows extracellular condensed DNA in the middle and future posterior of one-celled embryos (see Fig 4D).

[b] No polar bodies are seen by DIC in JU359 (characters 3-5). However, DAPI staining shows extracellular condensed DNA in the middle of one-celled embryos (see Fig. S8).

[c] PS1179 shows one (11/12) or two (1/12) PN. (see www.rhevolution.org).

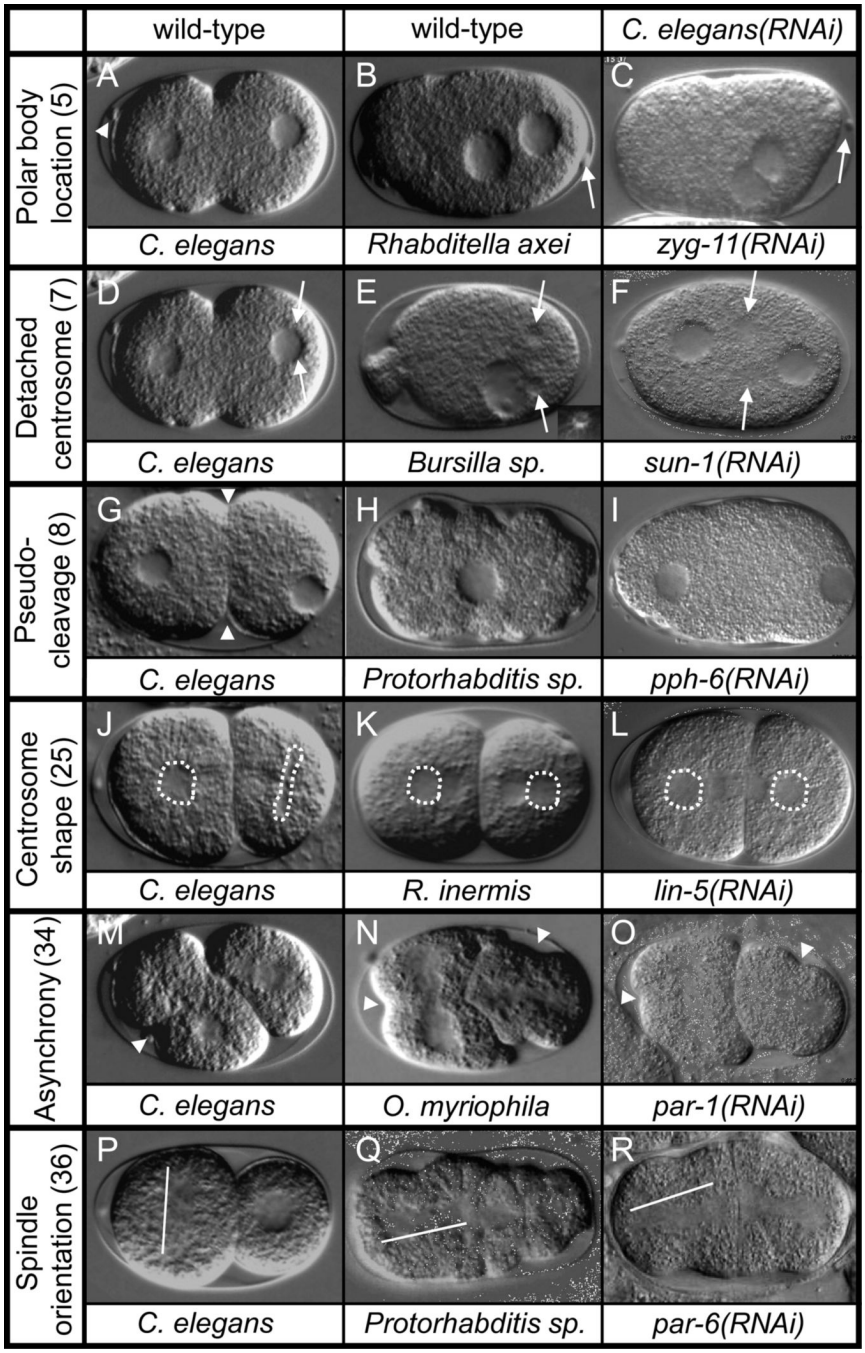

Figure 3. ***RNAi experiments in*** **C. elegans** ***mimic phenotypes in other species***

DIC images of *C. elegans* wild-type events (first column: A,D,G,J,M,P) compared to wild-type phenotypes of other rhabditid species (second column: B,E,H,K,N,Q) and phenotypes obtained in RNAi experiments in *C. elegans* (third column: C,F,I,L,O,R, pictures taken from phenobank.org or RNAi.org). All embryos are oriented with the anterior to the left. Characters are (character number from Fig. 2 in parentheses): Polar body location posterior (B, C; arrow) or anterior (A; arrowhead). Centrosomes (arrows) attached to pronucleus (initially not visible by DIC) (D) or detached from pronucleus (E, F) (inset in E: tubulin immunolabeling of a one-cell stage *Bursilla* sp. PS1179 embryo confirms presence of detached microtubule organizing centers). Pseudocleavage (arrowheads) present (G) or absent (H, I; note that contractility is

nevertheless present). Centrosome shape (dotted lines) different (J) or similar (K and L) in AB and P_1. Asynchronous (M) or synchronous (N, O) division of the AB and P_1 blastomeres (furrow ingression, representing the start of cytokinesis, is indicated with an arrowhead). Spindle orientation in AB (white line) perpendicular to (P) or along (Q, R) the AP axis.

Phenotype (character Nº)	Gene name	character Nº						Functional description
		5	7	8	25	34	36	
At least one polar body is seen in the posterior (5)	*zyg-11*	■		▒	▒	▒		ser/thr protein kinase
	elc-1	■			▒			elongin C ortholog
	mat-1	■						DNA-binding cell div. cycle control protein
Centrosome-like structures initially appear away from the pronucleus (7)	*zyg-12*		■					coiled-coil containing linker protein
	F40H6.6		■					unknown
	sun-1		■					spindle pole body protein
Pseudo-cleavage is absent (8)	*zyg-11*	▒		■	▒	▒		ser/thr protein kinase
	cye-1			■	▒	▒		G1/S specific cyclin E
	rsa-1			■	▒	▒		protein phosphatase 2 regulatory subunit
	hel-1			■		▒		ATP-dependent RNA helicase
	cyp-31A2			■		▒		cytochrome P450 subfamily
	spd-2			■				coiled-coil domain
	ruvb-1			■				DNA helicase
	cyk-4			■				Rho family GTPase activating protein
	ZK1127.5			■				RNA 3'-terminal phosphate cyclase
	pph-6			■				ser/thr specific protein phosphatase
The centrosomes have similar shapes after cytokinesis (25)	*zyg-11*	▒		▒	■	▒		ser/thr protein kinase
	cye-1			▒	■	▒		G1/S specific cyclin E
	rsa-1			▒	■	▒		protein phosphatase 2 regulatory subunit
	pkc-3				■	▒	▒	ser/thr protein kinase
	par-6				■	▒	▒	cell polarity protein, PDZ domain
	elc-1	▒			■			elongin C ortholog
	lin-5				■	▒		coiled-coil domain
	gpr-1/2				■	▒		GoLoco motif
	par-2				■	▒		cell polarity protein, RING domain
	par-5				■	▒		cell polarity protein, 14-3-3-family
	npp-1				■	▒		nuclear pore complex, p54 component
	nrs-1				■			Asparaginyl-tRNA synthetase
	ekl-1				■			unknown
	sur-6				■			ser/thr protein phophatase 2A, reg. subunit
	dyrb-1				■			Dynein-assoc. protein Roadblock
	cdc-37				■			cell division cycle 37 protein
	ruvb-2				■			DNA helicase TIP49, TBP interacting protein
	cyb-3				■			Cyclin B and related kinase-activating protein
	let-99				■			DEP domain
The second divisions are synchronous (34)	*zyg-11*	▒		▒	▒	■		ser/thr protein kinase
	rsa-1			▒	▒	■		G1/S specific cyclin E
	cye-1			▒	▒	■		protein phosphatase 2 regulatory subunit
	pkc-3				▒	■	▒	ser/thr protein kinase
	par-6				▒	■	▒	cell polarity protein, PDZ domain
	hel-1			▒		■		ATP-dependent RNA helicase
	cyp-31A2			▒		■		cytochrome P450 subfamily
	lin-5				▒	■		coiled-coil domain
	gpr-1/2				▒	■		GoLoco motif
	par-2				▒	■		cell polarity protein, RING domain
	par-5				▒	■		cell polarity protein, 14-3-3-family
	npp-1				▒	■		nuclear pore complex, p54 component
	par-3					■	▒	cell polarity protein, PDZ domains
	puf-3					■		Translational repressor RNA binding protein
	lrg-1					■		truncated let-99 paralog
	F33G12.4					■		Leucine rich repeat
	taf-5					■		WD40 associated region in TFIID subunit
	mex-6					■		CCCH-type Zn-finger protein
	air-1					■		ser/thr protein kinase
	F54B3.3					■		AAA+-type ATPase
	par-1					■		ser/thr protein kinase
The AB spindle is oriented along the long axis of the embryo (36)	*pkc-3*				▒	▒	■	ser/thr protein kinase
	par-6				▒	▒	■	cell polarity protein, PDZ domain
	par-3					▒	■	cell polarity protein, PDZ domains

Figure 4. *Sets of* C. elegans genes which, when compromised by RNAi, result in phenotypes seen in wild-type development of other rhabditid species

For six characters which differ between *C. elegans* and other rhabditid species, the genes which result in a similar phenotype in *C. elegans* upon RNAi knockdown are given (black boxes). These gene sets represent members of molecular modules that we hypothesize to underlie the respective phenotype. RNAi knockdown of several genes gives rise to other phenotypes, among them phenotypes resembling other characters in this table (grey boxes).

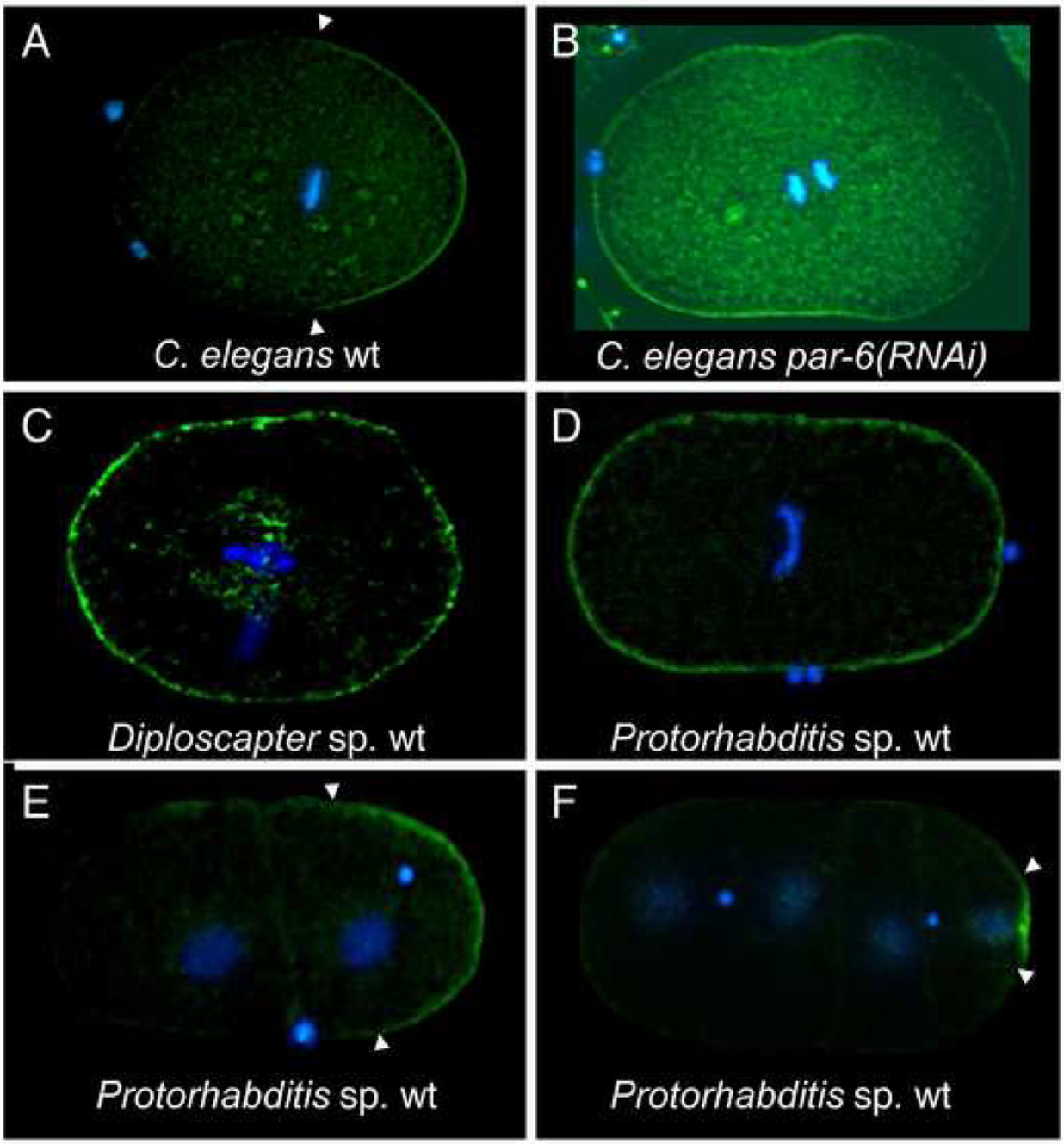

Figure 5. ***Novel PAR-1 localization in species of the*** **Protorhabditis** ***group***

Fluorescent staining of embryos with PAR-1 antibodies (green) and DAPI (blue). (A) PAR-1 localizes exclusively to the posterior half of the cortex in wild type *C. elegans* one-cell stage embryos (Kemphues, 2000). (B) PAR-1 localizes all around the cortex in a one-celled *C. elegans par-6(RNAi)* embryo (Guo and Kemphues, 1996), which ultimately leads to the ectopic spindle rotation in AB and the four-cells-in-a-row phenotype. (C,D) PAR-1 localizes all around the cortex at the one-cell stage in *Diploscapter* sp. (JU359) and *Protorhabditis* sp. (JB122) embryos. (E, F) During the two-cell (E) and four-cell (F) stage in *Protorhabditis* sp. (JB122), PAR-1 becomes asymmetrically localized in the germline precursor P_1 and P_2, just like in *C. elegans* (Guo and Kemphues, 1996).